CONFIDENTIAL X-67-64584 Copy 414
X-67-64584 RM L57J29

NACA RM L57J29

NACA

Declassified by authority of NASA
Classification Change Notices No. 212
Dated **
31 MAR 1971

RESEARCH MEMORANDUM

SOME EFFECTS OF REYNOLDS NUMBER ON THE STABILITY OF A SERIES OF FLARED-BODY AND BLUNTED-CONE MODELS AT MACH NUMBERS FROM 1.62 TO 6.86

By Alan B. Kehlet

Langley Aeronautical Laboratory
Langley Field, Va.

CLASSIFICATION CHANGED
UNCLASSIFIED
By Authority of TD 71-118 Date 29 JAN 1971

CLASSIFIED DOCUMENT
This material contains information affecting the National Defense of the United States within the meaning of the espionage laws, Title 18, U.S.C., Secs. 793 and 794, the transmission or revelation of which in any manner to an unauthorized person is prohibited by law.

NATIONAL ADVISORY COMMITTEE FOR AERONAUTICS

WASHINGTON

January 7, 1958

CONFIDENTIAL

THIS PAGE IS UNCLASSIFIED

ERRATA

NACA Research Memorandum L57J29

By Alan B. Kehlet
January 1958

Page 8: The last two sentences in the second complete paragraph should be corrected as follows:

"For model 6 a value of C_{m_q} of about -3 was calculated by using Newtonian theory. This is about 1/3 to 1/6 of the experimental values."

Pages 12 to 14: In table II, all values for C_{m_α} and $C_{m_q} + C_{m_{\dot{\alpha}}}$ (columns 6 and 7) should be negative in agreement with figures 6 and 7.

THIS PAGE IS UNCLASSIFIED Issued 8-18-58

DECLASSIFIED

CONFIDENTIAL

NATIONAL ADVISORY COMMITTEE FOR AERONAUTICS

RESEARCH MEMORANDUM

SOME EFFECTS OF REYNOLDS NUMBER ON THE STABILITY OF A SERIES OF FLARED-BODY AND BLUNTED-CONE MODELS AT MACH NUMBERS FROM 1.62 TO 6.86

By Alan B. Kehlet

SUMMARY

An investigation of some effects of Reynolds number on the stability of a series of flared-body and blunted-cone models at Mach numbers from 1.62 to 6.86 has been conducted in three Langley wind tunnels. The Reynolds number range covered was from 0.51×10^6 per foot to 24.0×10^6 per foot. The results showed that Reynolds number had a pronounced effect on the static stability of the flared-body models at the lower Mach numbers. Increasing the flare length increased both the static stability and the damping in pitch. Addition of a transition strip increased flare effectiveness. The blunted-cone models tested only at a Mach number of 6.86 exhibited better damping characteristics than the flared-body models at the same Mach number.

INTRODUCTION

Some effects of Reynolds number on the stability of a series of flared-body and blunted-cone models at Mach numbers from 1.62 to 6.86 are reported in this paper. The original purpose of these tests was to develop an air-flow indicator suitable for use on high Mach number pilotless aircraft; however, since a wide range of Reynolds numbers was covered, the data were deemed of interest as an indication of the characteristics of low-fineness-ratio flared-body and blunted-cone ballistic missiles.

During entry into the earth's atmosphere, a ballistic missile traverses a wide range of Mach numbers and Reynolds numbers. It is desirable that the missile be statically and dynamically stable at all Mach numbers and Reynolds numbers in order to reduce miss distances and high local heating in regions other than the nose. Flared-body configurations

CONFIDENTIAL

have attracted interest because of their stability in pitch and yaw at supersonic speeds (see ref. 1) and also because the flare offers advantages from a heating standpoint over conventional fins. The data of reference 1 show, however, that shock-wave—boundary-layer interaction tends to separate the flow from the junction of a flare with the body of the missile. It is known that separation affects the lift and static stability of a flared-body missile (ref. 2); however, little is known about the effect of separation on the damping.

These tests were conducted in three Langley wind tunnels by using a single-degree-of-freedom, free-oscillation technique and covered Mach number and Reynolds number ranges of 1.62 to 6.86 and 0.51×10^6 to 24.0×10^6, respectively. These results are limited in that force data were not obtained and, therefore, center-of-pressure locations cannot be determined.

SYMBOLS

A	base area of model 1, sq ft
I	moment of inertia, in pitch or yaw, slug-ft^2
P	period of oscillation, sec
R	Reynolds number per foot
$T_{1/2}$	time to damp to one-half amplitude, sec
V	velocity, ft/sec
c.g.	center of gravity
d	base diameter of model 1, ft
q	dynamic pressure, lb/sq ft; pitching velocity, radians/sec
t	time, sec
α	angle of attack, deg
β	angle of sideslip, deg

C_{m_α} static stability parameter about center of gravity,

$$-\frac{4\pi^2 I}{qAdP^2}, \text{ per radian}$$

$C_{m_{\frac{qd}{2V}}} + C_{m_{\frac{\dot{\alpha}d}{2V}}}$ damping-in-pitch parameter about center of gravity,

$$-\frac{4I(0.693)V}{qAd^2T_{1/2}}, \text{ per radian}$$

A dot over a symbol denotes the derivative with respect to time.

MODELS, TEST TECHNIQUE, AND TEST FACILITIES

Models

Side-view drawings of the models (bodies of revolution) are shown in figure 1. The flared-body models consisted of an ogive or a hemispherical nose section, a $1\frac{1}{2}$- caliber cylinder, and a cone frustum tail having a semiangle of 20°. The cone frustum varied in length from about $1\frac{1}{2}$ to $1\frac{3}{4}$ calibers. The diameter of the cylindrical section was 1 inch. One of the cone-shape models consisted of a blunted 10.7° cone; the others, an ogive nose section followed by a cone frustum having a semiangle of about 8°.

Each model was mass balanced so that the center-of-gravity station corresponded to the pivot line of the sting mechanism. The static-stability and damping-in-pitch data presented herein are referenced to the center-of-gravity position shown in figure 1. Mass characteristics of each model are given in table I.

Test Technique

A photograph of a typical wind-tunnel setup is shown in figure 2. Measurements of angle of attack and angle of sideslip were made by mounting the various models on the sting mechanism of a standard NACA air-flow-direction pickup (ref. 3). This mechanism allowed the models to oscillate in both the angle-of-attack and the angle-of-sideslip planes. The tests were analyzed by using a single-degree-of-freedom, free-oscillation technique. At each test condition, the model was held in an out-of-trim position in the angle-of-attack plane and then quickly released. From the resulting motions, the static stability C_{m_α}

was determined from the periods of the oscillations and the damping in pitch $C_{m_q} + C_{m_{\dot{\alpha}}}$ from the time to damp to one-half amplitude. (See section entitled "Symbols.")

Recording equipment consisted essentially of standard NACA FM telemeter components. The variable-inductance pickoff coils of the pickup channels were connected to an oscillator; the oscillator output was heterodyned and fed into a frequency discriminator connected to a recording oscillograph.

Test Facilities

The models were tested in three Langley wind tunnels at Mach numbers of 1.62, 2.62, 4.06, and 6.86 with Reynolds number variations at each Mach number. The model test ranges for each Mach number are given in table II.

Tests at Mach numbers of 1.62 and 2.62 were conducted in the Langley 9-inch supersonic tunnel. This tunnel is a continuous-operation complete-return type in which the absolute stagnation pressure may be varied and controlled from about 1/10 atmosphere to about 4 atmospheres. The stagnation temperature and dewpoint may also be varied and controlled. The Mach number is varied by interchanging nozzle blocks which form test sections approximately 9 inches square.

Tests at a Mach number of 4.06 were conducted in the Langley 9- by 9-inch high Mach number jet. A description and a calibration for this facility are given in reference 4.

Tests at a Mach number of 6.86 were conducted in the Langley 11-inch hypersonic tunnel. This tunnel is equipped with a single-step two-dimensional nozzle which is constructed of Invar and operates at an average Mach number of 6.86. There exists no published calibration for the Invar nozzle. More detailed information concerning this test facility may be found in reference 5.

ACCURACY

The probable uncertainties in the test data due to the accuracy of the recording equipment and to the technique used in each tunnel are listed in the following table:

Mach number	Accuracy		
	M	R per foot	q, lb/sq ft, percent
1.62	±0.01	$\pm 0.01 \times 10^6$	±1
2.62	.01	.01	1
4.06	.04	.30	3
6.86	.10	.30	10

Because of the original purpose of the investigation, only qualitative results were required from the tests conducted at M = 4.06 and 6.86. Tests at these two Mach numbers were made before the Mach number and settling-chamber stagnation temperature had stabilized; hence, the poor accuracy.

From the periodic calibration of the sting mechanism during the tests, the absolute value of angle of attack and angle of sideslip is estimated to be 0.20° at all Mach numbers.

RESULTS AND DISCUSSION

The test results for each model at all Reynolds numbers tested are given in table II. Representative parts of the data are presented in figures 3 to 7, and schlieren photographs of some of the tests are shown in figures 8 to 10.

General Data Characteristics

Examples of the resulting motions for which the damping parameter $C_{m_q} + C_{m_{\dot{\alpha}}}$ was obtained and those for which it was not obtained are shown in figures 3 and 4, respectively. In figure 3 only the angle-of-attack data are shown, since, throughout the test time, the angles of sideslip were zero. Values of $C_{m_q} + C_{m_{\dot{\alpha}}}$ were not obtained from the model motions shown in figure 4 because of either undamped oscillations or motions in both planes. The reason for the motions in both planes is unknown. At Mach numbers and Reynolds numbers at which this type of motion occurred, it may be that at angles of attack the flow along the body was no longer axially symmetric and a vortex type of flow was established. Releasing the models at lower initial angles in some cases reduced or eliminated the motions in the sideslip plane. Release-mechanism and internal-sting interferences are also possible causes. Calculating the resultant of the two motions resulted in most cases in

a "beat" type of damping with little or no change in frequency. The frequency of the angle-of-attack oscillation was used to calculate static stability when results as shown in figure 4 were obtained.

The variation of half-periods and amplitude ratios with time for model 1 at a Mach number of 4.06 is shown in figure 5. It may be noted that the periods and the logarithmic decrements (and therefore the static stability and the damping parameter, respectively) are nonlinear with angle of attack. The nonlinearity is a function of the flow separation at the body-flare junction. The amount of flow separation of model 1 at a Mach number of 4.06 can be seen in figure 10. With pronounced flow separation (figs. 8 and 9), the static stability and the damping in pitch decrease as the angle of attack is increased. Tests conducted on a cone-cylinder with a large base flare (ref. 2), show that with pronounced flow separation, nonlinearities in normal force and center of pressure with angle of attack occurred in the same manner as nonlinearities in static-stability and the damping-in-pitch parameter with angle of attack occurred in the present test.

Static Stability

The variations of the static stability parameter C_{m_α} as a function of Reynolds number at the several Mach numbers are shown in figure 6. The static stability data were calculated for the angle-of-attack range given in table II. Reference to this range is of paramount importance when comparing models. Also included in figure 6 are the flared-body-model data of references 6 to 8, interpolated to conform to the same cylinder and flare lengths and center-of-gravity positions as the present models, and Newtonian theory C_{m_α} for model 6. The reference models had surface roughness applied to the nose tips to reduce flow separation at the body-flare junction.

At Mach numbers of 1.62 and 2.62, Reynolds number (over the range covered) has a pronounced effect on the static stability. At $M = 1.62$, increasing R from about 0.5×10^6 to 2.0×10^6 decreases C_{m_α} to approximately 1/3 that at $R = 0.5 \times 10^6$. All models tested were statically stable at $M = 1.62$ although schlieren photographs at this Mach number (fig. 8) show extensive separation over the flare at the lowest R tested (highest value of C_{m_α}). At $M = 2.62$, variations in R produced results similar to those at $M = 1.62$, except that as R decreased, C_{m_α} increased to a peak value and then sharply decreased. Tests conducted at lower values of R than shown in figure 6(b) (table II)

DECLASSIFIED

resulted in model static and dynamic instabilities. Schlieren photographs of models 1, 2, 3, and 5 at $M = 2.62$ are shown in figure 9. It may be noted in figure 9 that at values of R for which the models are unstable, the shock formations (except for model 1) are ragged and do not have the $M = 2.62$ shock angles. Since models 1 and 5 had the same nose shape, the reason that model 1 does not have the same shock formation as model 5 at the low Reynolds numbers is unknown.

Addition of a transition strip to model 1 (model 2) increased the flare effectiveness (see fig. 6(b)). Model 3 data were not faired because of the low oscillation amplitude.

An increase in static stability with a decrease in Reynolds number was also noted in tests conducted on an ogive-cylinder body at $M = 1.98$ and presented in reference 9. The tests at $M = 1.98$ were made at Reynolds numbers of 1.56×10^6 per foot, and 4.68×10^6 per foot which are within the changing C_{m_α} range shown in figures 6(a) and 6(b).

Over the Reynolds number range covered at $M = 4.06$ and 6.86, Reynolds number had little effect on the static stability. It may be that the Reynolds numbers tested were not low enough to determine whether C_{m_α} varied in a manner similar to $M = 1.62$ and $M = 2.62$; however, schlieren photographs of models 1 and 5 at $M = 6.86$ (fig. 10) show extensive flow separation over the flare similar to the lower Reynolds number tests at $M = 1.62$ (fig. 8). The blunted-cone models (tested only at $M = 6.86$) were designed and built as a result of the flared-body tests. It was believed that the cone models would be less sensitive to Reynolds number effects than the flared-body models. The blunted-cone model (model 6) exhibited a degree of static stability between the short flare model (model 1) and the long flare model (model 5). The ogive nose-cone models exhibited less static stability than the short flare model.

It may be noted that throughout the Mach number and Reynolds number ranges, increasing the flare length increased the static stability. At Mach numbers where comparisons could be made, the results of the present tests and the results of references 6 to 8 are in good agreement.

Damping in Pitch

The variation of the damping-in-pitch parameter $\left(C_{m_q} + C_{m_{\dot{\alpha}}}\right)$ with Reynolds number and as a function of Mach number is shown in figure 7. Because the damping varied with amplitude in most cases and because of possible friction effects in the sting mechanism, the results presented

in figure 7 should be treated as qualitative data. Where there were oscillations in both planes such that as α damped β diverged (fig. 4), no values of the damping parameter were obtained.

The friction in the sting mechanism and, consequently, the amount of artificial damping, is a function of the model drag. Since the differences in total drag at a constant Mach number are small for all the models in the present test, comparisons of the damping in pitch between the models may be made even if the absolute magnitude is in error.

Generally, increasing the flare length on the flared-body models resulted in increased values of $C_{m_q} + C_{m_{\dot{\alpha}}}$. Models 1 and 5 when tested at $M = 6.86$ were instrumented in one plane only although they were allowed to oscillate in both planes. Model 5 at $M = 6.86$ exhibited a value of zero damping in pitch at the amplitude shown in table II. Model 1 exhibited damping in the α-plane at this Mach number, but visual observation indicated that the model may have been continuously oscillating in the β-plane; for this reason, the damping results of model 1 at $M = 6.86$ are not presented. The cone models ($M = 6.86$) exhibited good damping characteristics at Reynolds numbers where the flared-body models were believed to have zero values of damping in pitch. For model 6 a value of C_{m_q} of about 40 was calculated by using Newtonian theory. This is from two to four times greater than experimental values.

Because of insufficient data, effects of Reynolds number on the damping in pitch can not be ascertained. It is of interest to note that at a constant Reynolds number, the presence of static stability does not necessarily indicate the presence of damping in pitch; for example, model 3 at $M = 2.62$ and model 5 at $M = 6.86$.

CONCLUDING REMARKS

An investigation of some effects of Reynolds number on the stability of a series of flared-body and blunted-cone models at Mach numbers from 1.62 to 6.86 has been conducted. The Reynolds number range varied from 0.51×10^6 per foot to 24.0×10^6 per foot.

Reynolds number variation had a pronounced effect on the static stability of the flared-body models at the lower Mach numbers. At a Mach number of 2.62, where a "critical" range of Reynolds numbers was covered, decreasing the Reynolds number increased the static stability to a peak value; a further reduction in Reynolds number resulted in

static and dynamic instabilities. At a Mach number of 1.62, over the range of Reynolds numbers covered, decreasing the Reynolds number increased the static stability. Reynolds number variations had little effect on the static stability at Mach numbers of 4.06 and 6.86 probably because of the small range covered. Increasing the flare length increased the value of the static stability and the damping in pitch. The addition of a transition strip increased the flare effectiveness.

Because of possible friction effects in the sting mechanism, the damping-in-pitch results are to be treated as qualitative data. However, since the friction is a function of model drag and at a constant Mach number the differences in drag are small, comparisons of models at a constant Mach number may be made. The cone models tested only at a Mach number of 6.86 exhibited better damping characteristics than the flared-body models at the same Mach number.

Langley Aeronautical Laboratory,
National Advisory Committee for Aeronautics,
Langley Field, Va., October 8, 1957.

REFERENCES

1. Eggers, A. J., Jr., and Syvertson, Clarence A.: Experimental Investigation of a Body Flare for Obtaining Pitch Stability and a Body Flap for Obtaining Pitch Control in Hypersonic Flight. NACA RM A54J13, 1955.

2. Dennis, David H., and Syvertson, Clarence A.: Effects of Boundary-Layer Separation on Normal Force and Center of Pressure of a Cone-Cylinder Model With a Large Base Flare at Mach Numbers From 3.00 to 6.28. NACA RM A55H09, 1955.

3. Ikard, Wallace L.: An Air-Flow-Direction Pickup Suitable for Telemetering Use on Pilotless Aircraft. NACA TN 3799, 1956. (Supersedes NACA RM L53K16, 1954.)

4. Ulmann, Edward F., and Lord, Douglas R.: An Investigation of Flow Characteristics at Mach Number 4.04 Over 6- and 9-Percent-Thick Symmetrical Circular-Arc Airfoils Having 30-Percent-Chord Trailing-Edge Flaps. NACA RM L51D30, 1951.

5. McLellan, Charles H., Williams, Thomas W., and Beckwith, Ivan E.: Investigation of the Flow Through a Single-Stage Two-Dimensional Nozzle in the Langley 11-Inch Hypersonic Tunnel. NACA TN 2223, 1950.

6. Lavender, Robert E.: Normal Force, Pitching Moment, and Center of Pressure of Eighty Cone-Cylinder-Frustum Bodies of Revolution at Mach Number 1.50. Rep. 6R3N3, Ord. Missile Labs., Redstone Arsenal (Huntsville, Ala.), Apr. 5, 1956.

7. Sims, Joseph L., and Henderson, James H.: Normal Force, Pitching Moment, and Center of Pressure of Eighty Cone-Cylinder-Frustum Bodies of Revolution at Mach Number 2.81. Rep. 6R3N2, Ord. Missile Labs., Redstone Arsenal (Huntsville, Ala.), Mar. 28, 1956.

8. Henderson, James H., and Sims, Joseph L.: Normal Force, Pitching Moment and Center of Pressure of Eighty Cone-Cylinder-Frustum Bodies of Revolution at Mach number 4.04. Rep. 6R3N1, Ord. Missile Labs., Redstone Arsenal (Huntsville, Ala.), Mar. 1, 1956.

9. Perkins, Edward W., and Jorgensen, Leland H.: Comparison of Experimental and Theoretical Normal-Force Distributions (Including Reynolds Number Effects) On An Ogive-Cylinder Body at Mach Number 1.98. NACA TN 3716, 1956. (Supersedes NACA RM A54H23, 1954.)

DECLASSIFIED

TABLE I.- MODEL MASS CHARACTERISTICS

Model number	Moment of inertia, slug-ft^2	Weight, lb
1	0.3270×10^{-4}	0.1687
2	.3280	.1709
3	.2936	.1645
4	.3495	.1687
5	.4111	.1773
6	.2956	.1420
7	.3272	.1702
8	.3820	.1627

TABLE II.- MODEL TEST RESULTS

(a) M = 1.62

Model number	R per ft	q, lb/sq ft	P, sec	$T_{1/2}$, sec	C_{m_α} per radian	$C_{m_q} + C_{m_{\dot{\alpha}}}$ per radian	α, deg
1	0.51×10^6	104	0.058	0.360	2.45	19.43	[a]±5.0
	.98	197	.049	.205	1.82	18.02	5.0
	1.90	383	.055	-----	.74	-----	[a]5.0
4	0.51×10^6	104	0.048	0.255	3.83	29.32	±4.0
	.98	196	.041	.155	2.79	25.60	4.5
5	0.51×10^6	104	0.050	-----	4.15	-----	[a]±5.0
	1.91	383	.043	-----	1.52	-----	[a]4.0

[a]Some β oscillations (see fig. 4).

DECLASSIFIED

TABLE II.- MODEL TEST RESULTS - Continued

(b) M = 2.62

Model number	R per ft	q, lb/sq ft	P, sec	$T_{1/2}$, sec	C_{m_α} per radian	$C_{m_q} + C_{m_{\dot{\alpha}}}$ per radian	α, deg
1	0.62×10^6	108	Statically and dynamically unstable neutral stability at α = 0				
	1.06	182					
	1.15	199	0.040	∞	2.70	0	±3.0
	1.34	232	.038	1.140	2.56	3.55	2.5
2	0.53×10^6	92	Statically and dynamically unstable neutral stability at α = 0				
	.57	100					
	.62	108	0.075	0.250	1.42	34.87	±5.0
3	1.08×10^6	187	0.034	∞	3.57	0	±1.5
	1.27	219	.030	∞	3.91	0	1.5
	1.53	266	.040	0.120	1.81	26.40	3.0
4	0.46×10^6	79	Statically and dynamically unstable				
	.63	107	Statically and dynamically unstable				
	.97	166	0.048	0.940	2.40	6.43	±4.5
	3.11	539	.042	-----	.97	----	[a]4.0
5	0.48×10^6	81	Statically and dynamically unstable				
	.68	116	0.059	1.52	2.67	6.69	[a]±5.0
	.97	165	.042	.81	3.71	8.83	3.5
	3.12	533	.038	----	1.40	----	[a]3.5

[a]Some β oscillations (see fig. 4).

TABLE II.- MODEL TEST RESULTS - Concluded

(c) M = 4.06

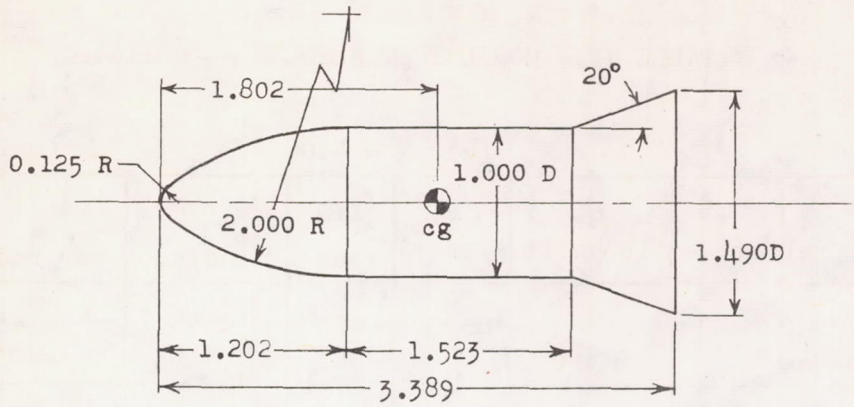
Model number	R per ft	q, lb/sq ft	P, sec	$T_{1/2}$, sec	C_{m_α} per radian	$C_{m_q} + C_{m_{\dot{\alpha}}}$ per radian	α, deg
1	17.2×10^6 24.0	1700 2380	0.030 .030	0.055 .032	0.56 .40	10.45 12.83	±5.0 5.0
2	24.0	2380	0.040	0.023	0.23	17.91	±5.0
3	24.0	2380	0.032	0.039	0.32	9.45	±5.0
5	17.2 24.0	1700 2380	0.022 .021	0.056 .039	1.31 1.03	12.91 13.24	±5.0 5.0

(d) M = 6.86

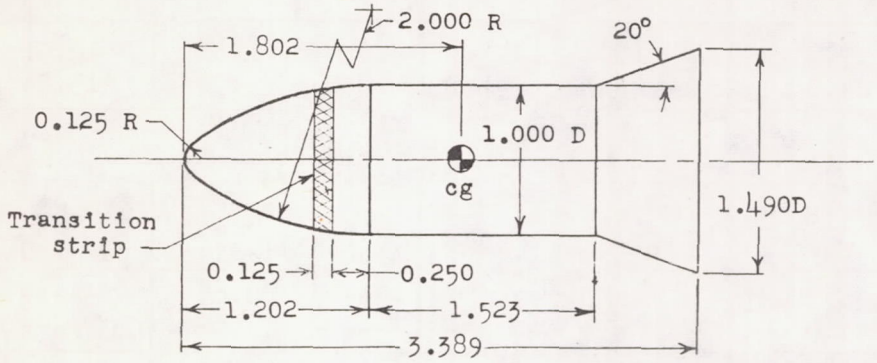
Model number	R per ft	q, lb/sq ft	P, sec	$T_{1/2}$, sec	C_{m_α} per radian	$C_{m_q} + C_{m_{\dot{\alpha}}}$ per radian	α, deg
1	3.10×10^6 4.40	480 630	0.054 .047	----- -----	0.61 .62	----- -----	[b]±5.0 [b]5.0
5	2.70 3.30 4.50	380 480 630	0.040 .037 .033	∞ ∞ ∞	1.78 1.64 1.57	0 0 0	±5 6 6
6	1.60 3.40	195 490	0.058 .039	0.419 .293	1.18 1.04	17.75 10.31	±5 5
7	1.60 3.00	200 485	0.152 .099	0.216 .191	0.19 .18	37.04 17.74	±5 5
8	1.50 3.10	200 490	0.102 .067	0.311 .187	0.48 .46	29.94 20.94	±5 5

[b]Damping characteristics questionable.

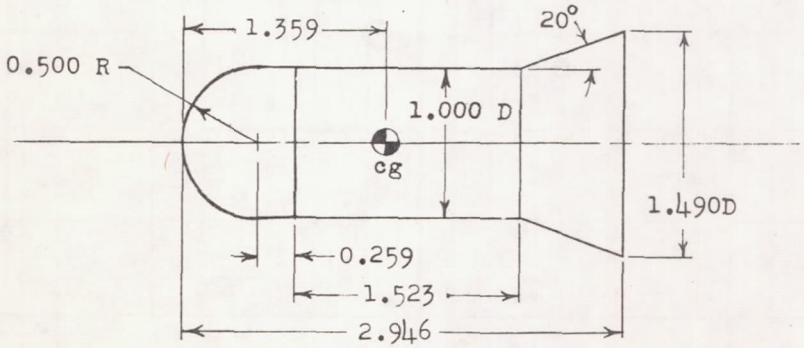
DECLASSIFIED



(a) Model 1.

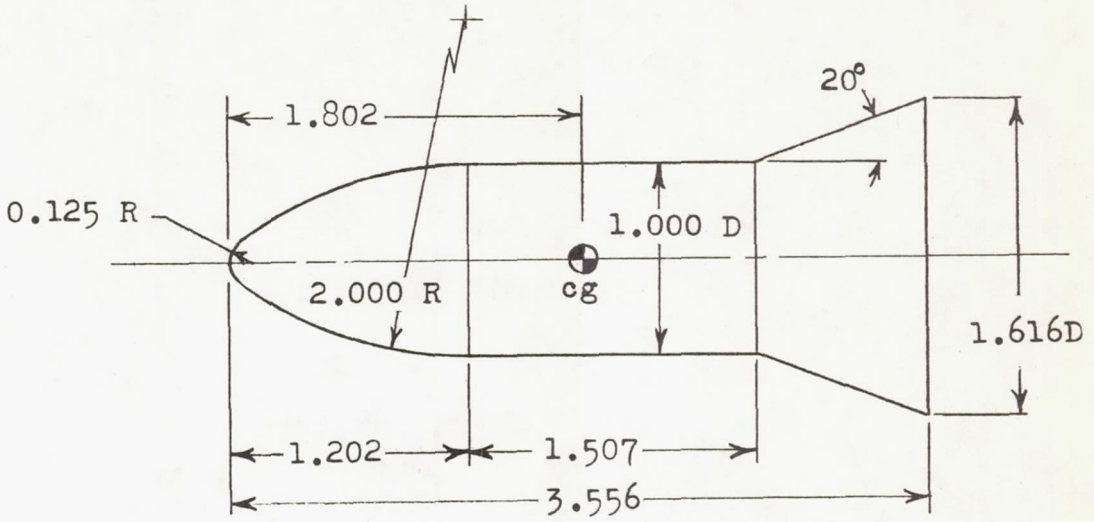


(b) Model 2.

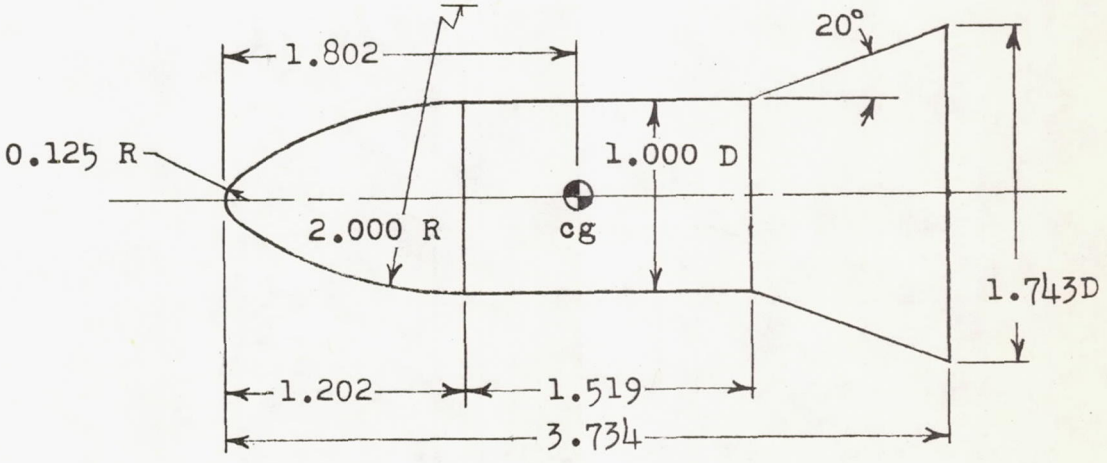


(c) Model 3.

Figure 1.- General arrangement of eight models. All dimensions in inches.



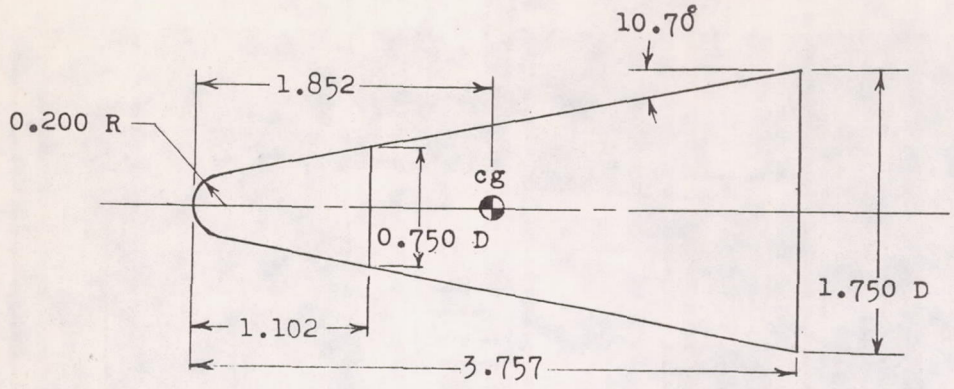
(d) Model 4.



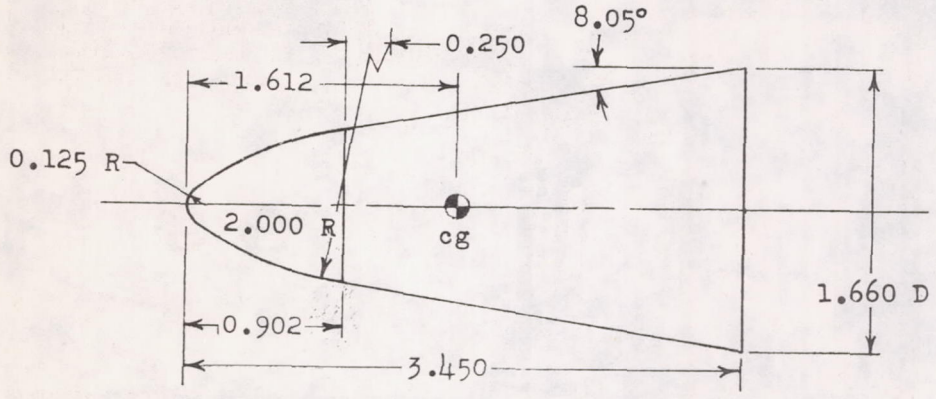
(e) Model 5.

Figure 1.- Continued.

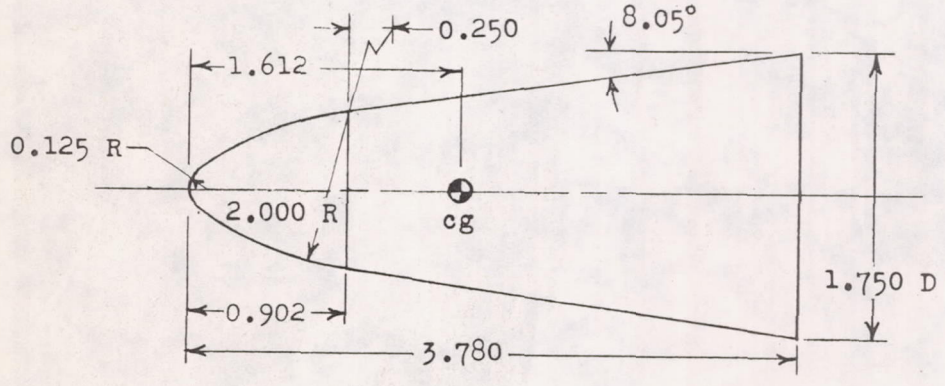
DECLASSIFIED



(f) Model 6.



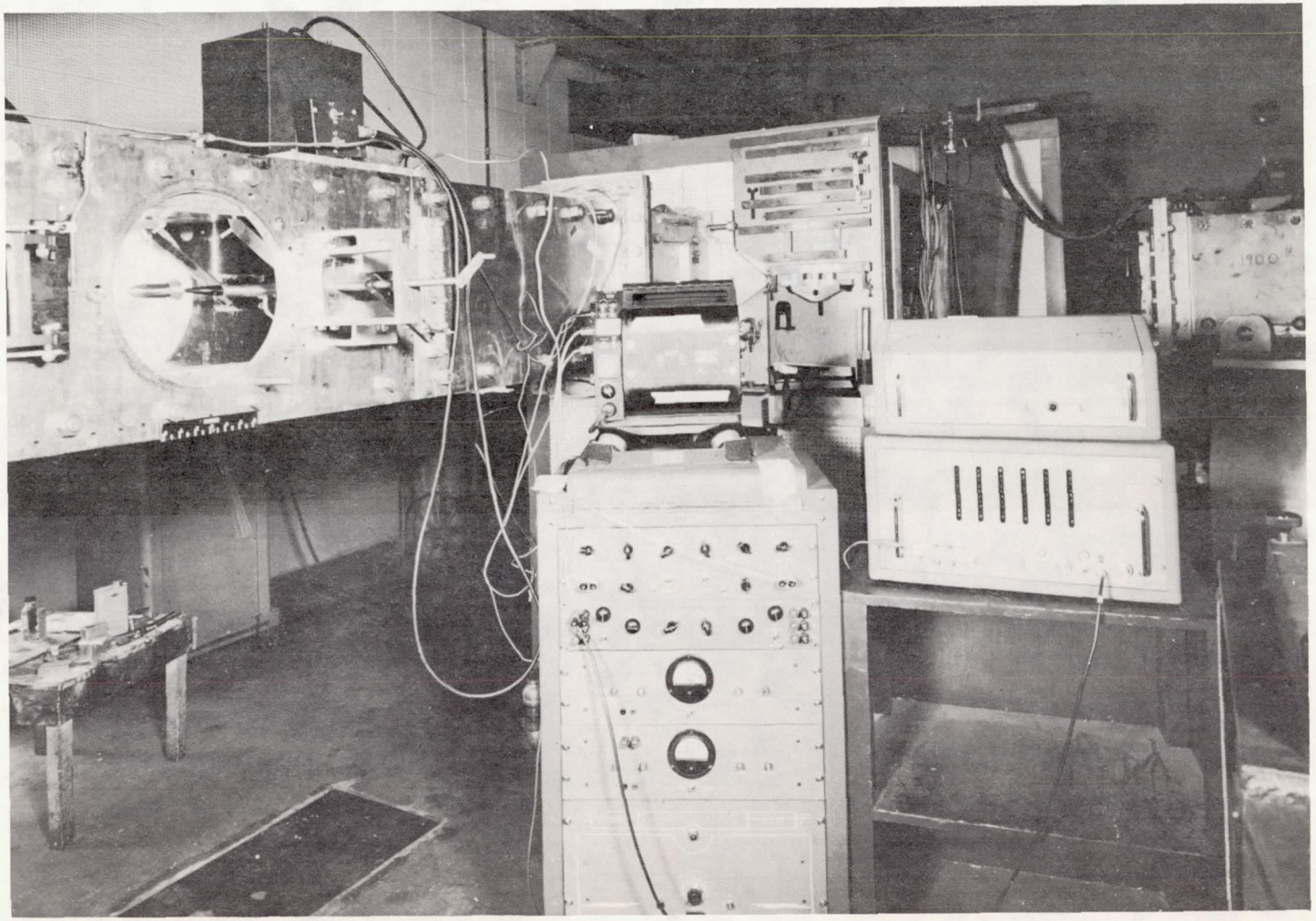
(g) Model 7.



(h) Model 8.

Figure 1.- Concluded.

CONFIDENTIAL

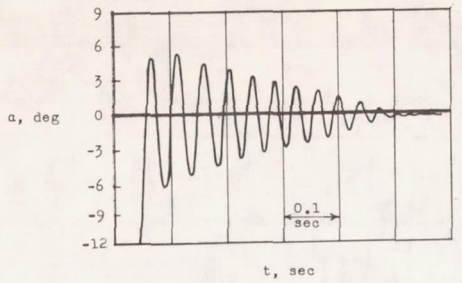


L-91919

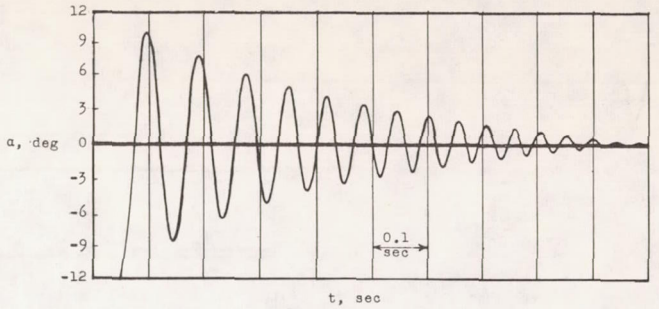
Figure 2.- Photograph of model, instrumentation, and typical wind-tunnel setup.

CONFIDENTIAL

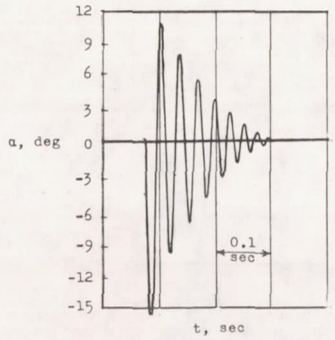
CONFIDENTIAL



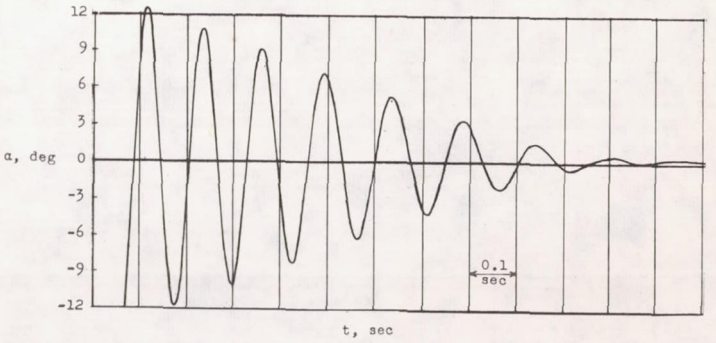
(a) Model 1; M = 1.62;
R = 0.98 × 10^6 per foot.



(b) Model 2; M = 2.62;
R = 0.62 × 10^6 per foot.



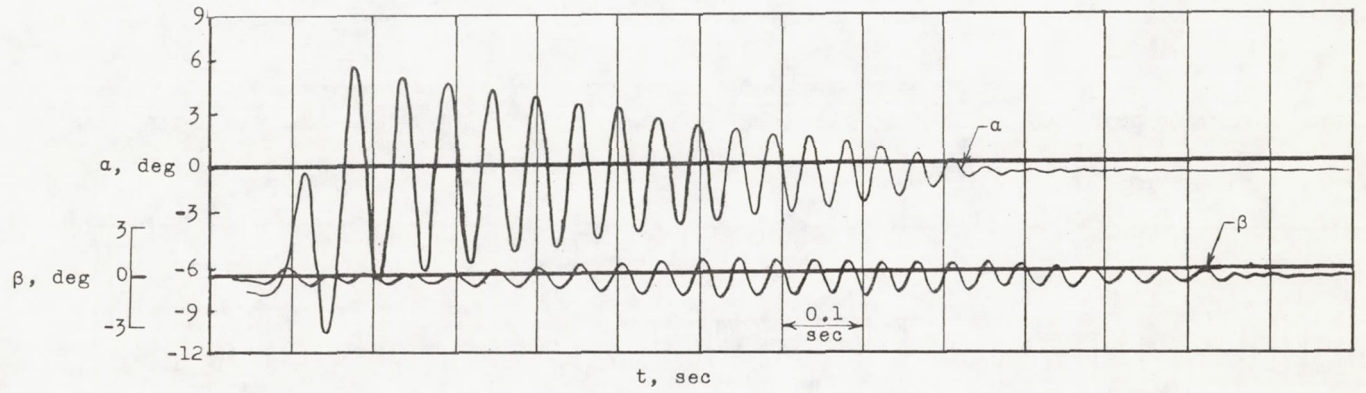
(c) Model 1; M = 4.06;
R = 17.2 × 10^6 per foot.



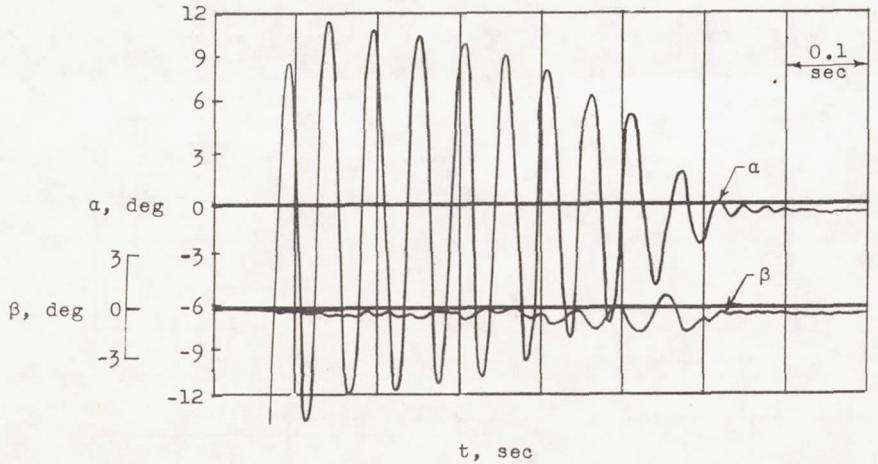
(d) Model 7; M = 6.86;
R = 1.60 × 10^6 per foot.

Figure 3.- Some time histories of motions for various models, Mach numbers, and Reynolds numbers, for which values of damping were obtained.

CONFIDENTIAL



(a) Model 1; M = 1.62; R = 0.51×10^6 per foot.

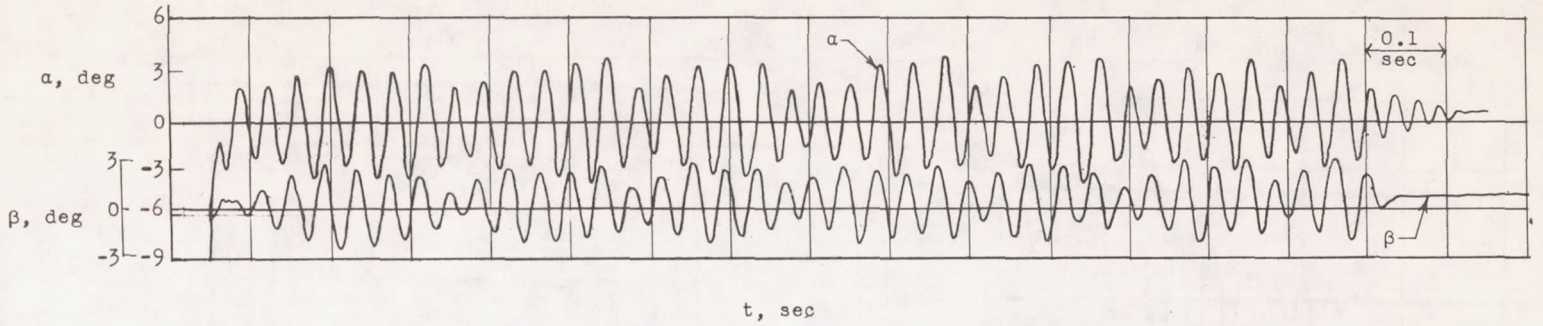


(b) Model 1; M = 1.62; R = 1.90×10^6 per foot.

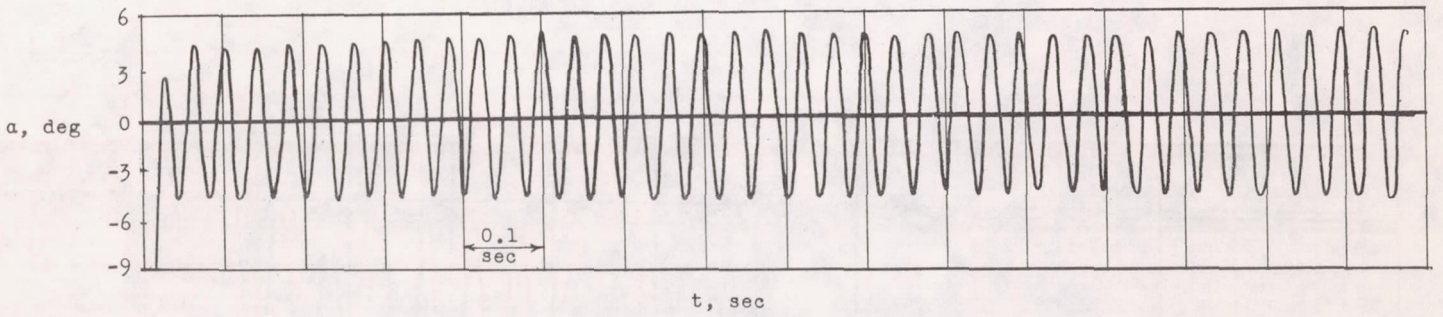
Figure 4.- Some time histories of motions for various models, Mach numbers, and Reynolds numbers, for which values of damping were not obtained.

CONFIDENTIAL

CONFIDENTIAL



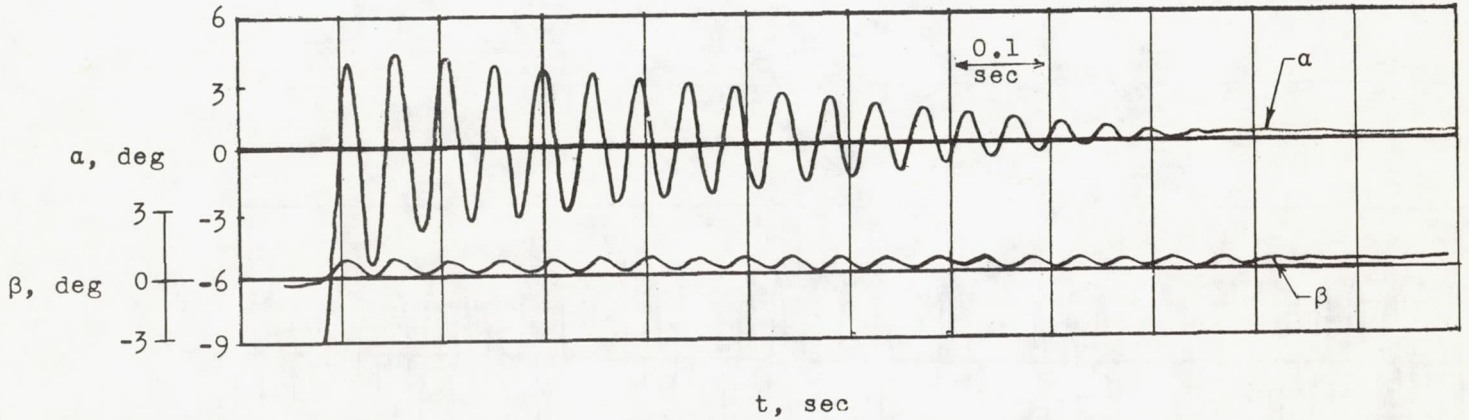
(c) Model 4; M = 2.62; R = 3.11×10^6 per foot.



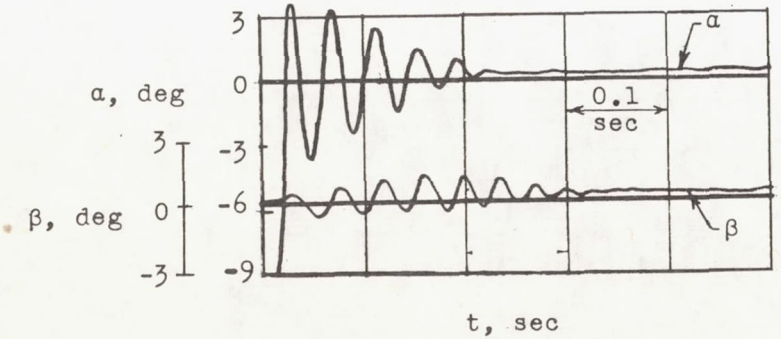
(d) Model 5; M = 6.86; R = 2.70×10^6 per foot.

Figure 4.- Continued.

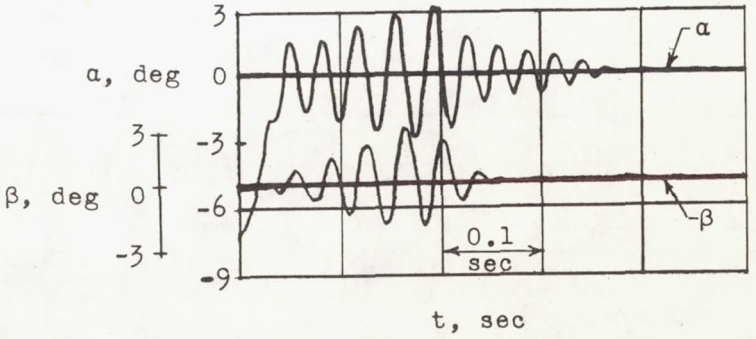
CONFIDENTIAL



(e) Model 5; M = 1.62;
R = 0.51 × 10^6 per foot.



(f) Model 5; M = 1.62;
R = 1.91 × 10^6 per foot.

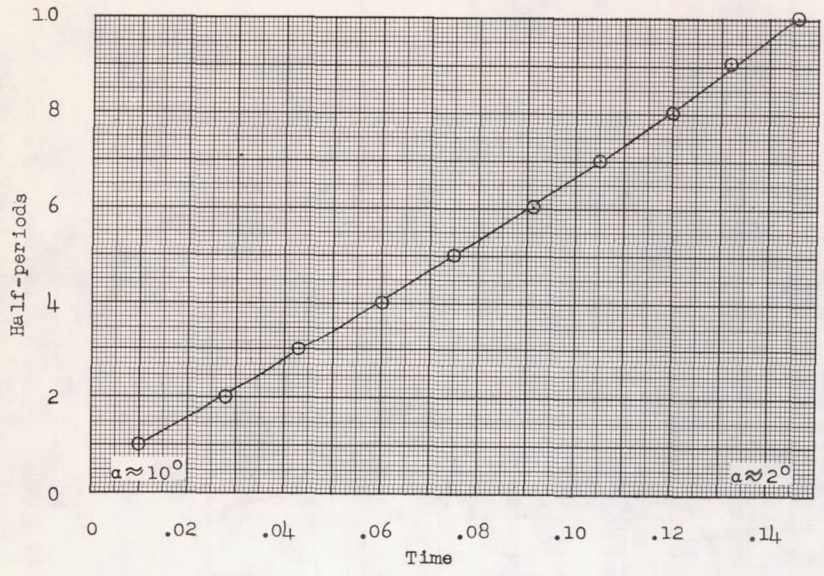


(g) Model 5; M = 2.62;
R = 3.12 × 10^6 per foot.

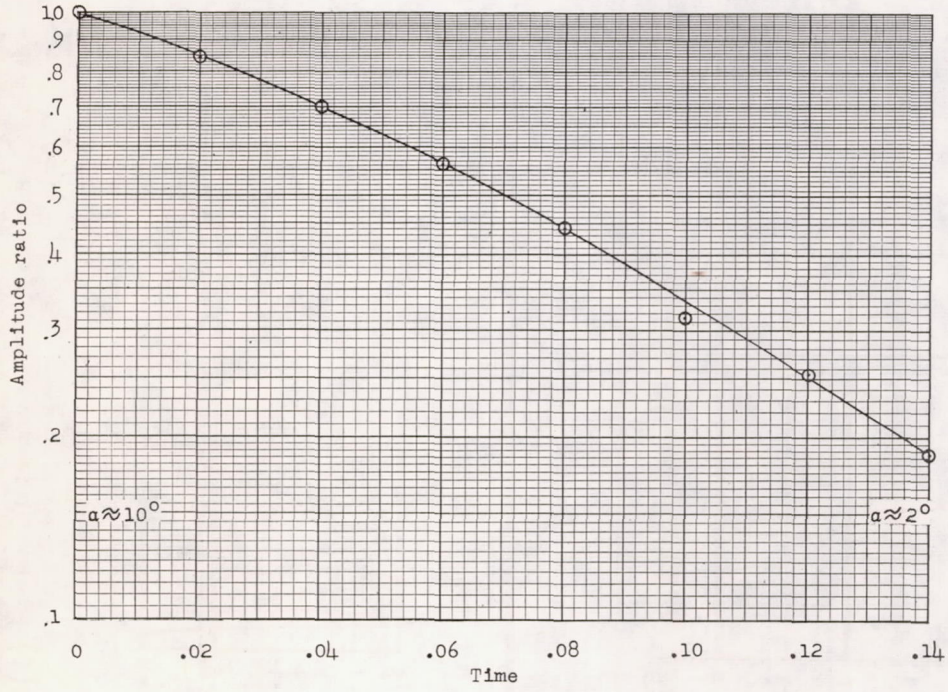
Figure 4.- Concluded.

CONFIDENTIAL

DECLASSIFIED

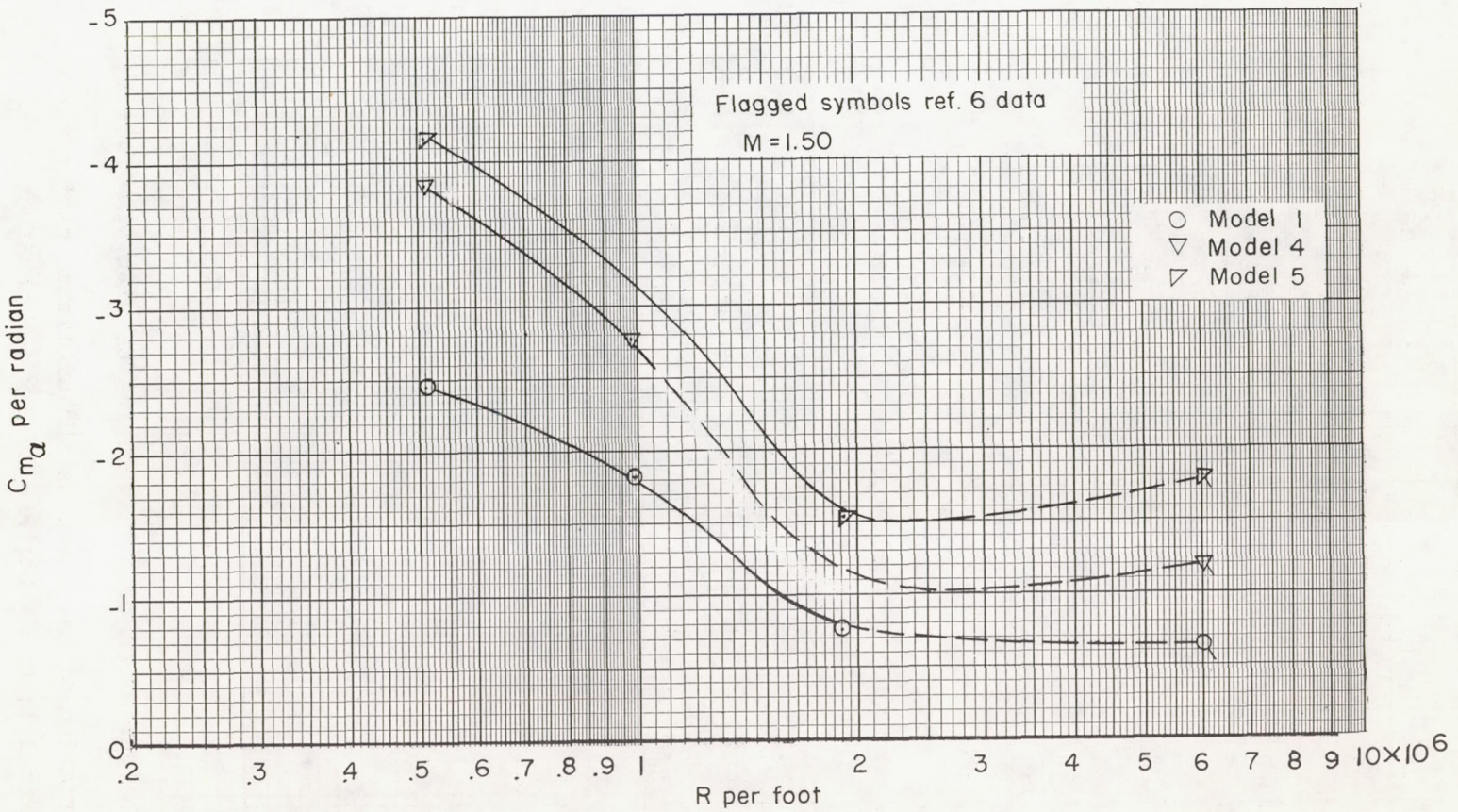


(a) Variation of half-periods with time.



(b) Variation of amplitude ratios with time.

Figure 5.- Variation of half-periods and amplitude ratios with time. Model 1; M = 4.06; R = 17.2×10^6 per foot.

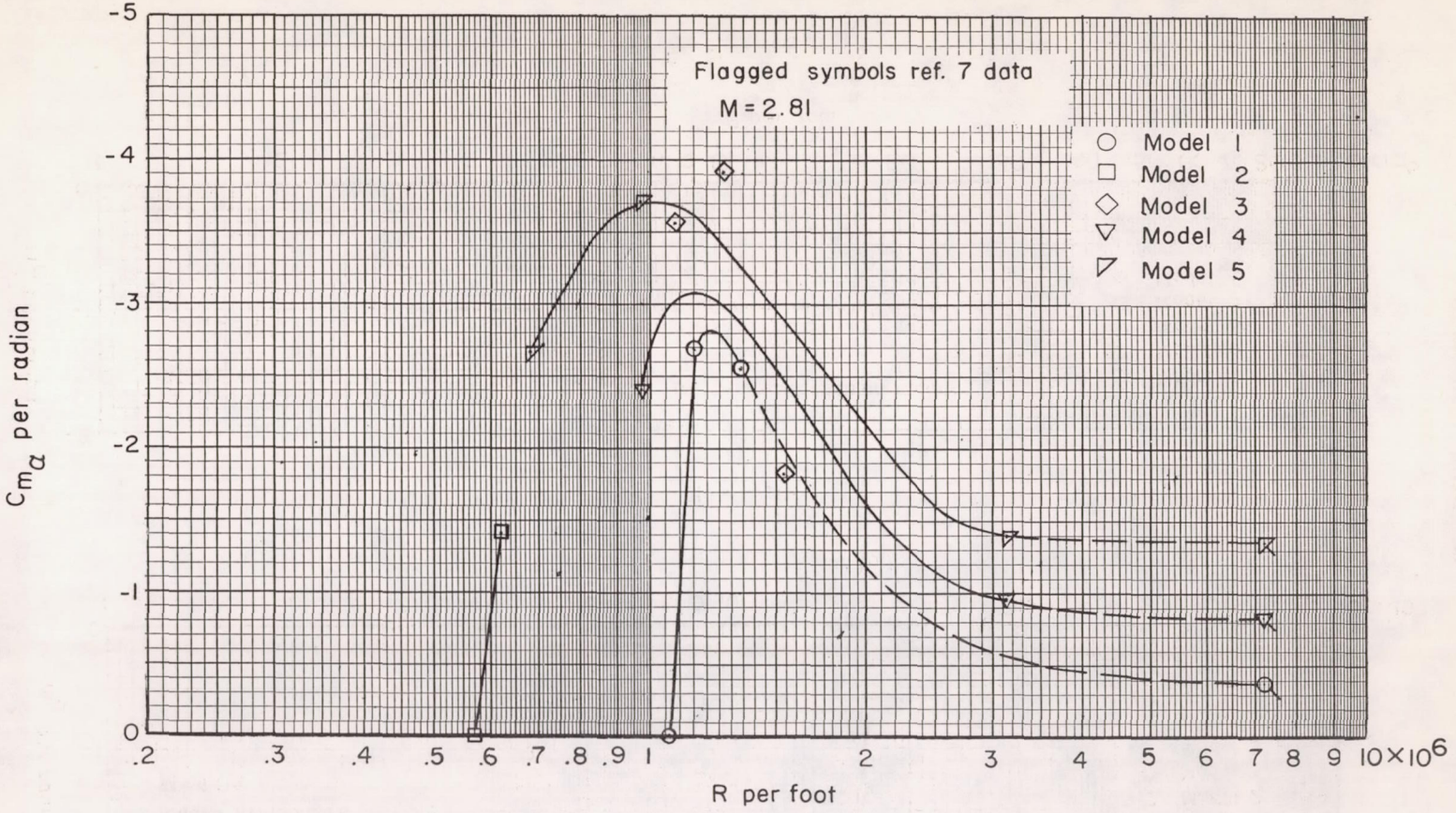


(a) M = 1.62.

Figure 6.- Variation of static stability parameter C_{m_α} as function of Reynolds number at M = 1.62, 2.62, 4.06, and 6.86. Reference area is base area of model 1.

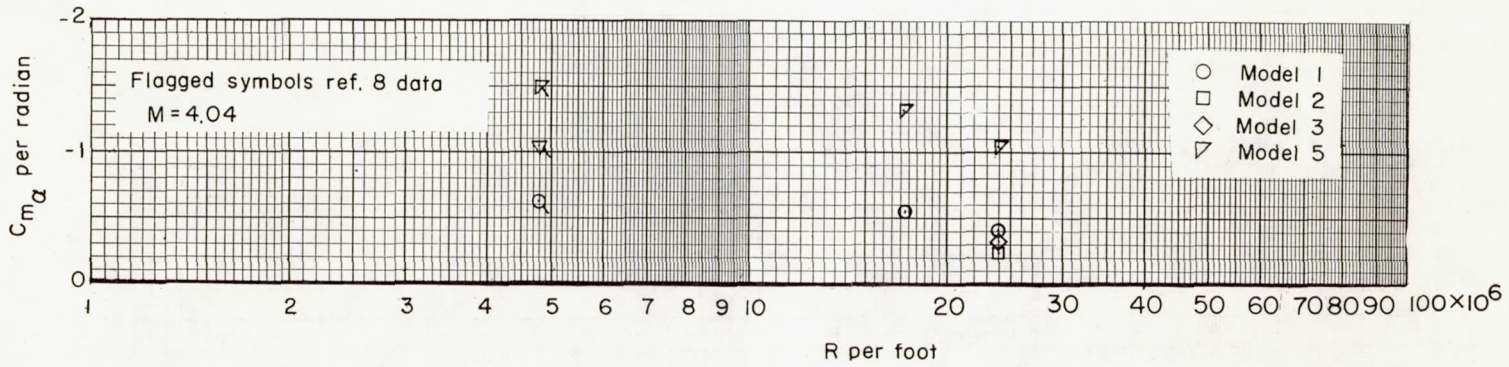
CONFIDENTIAL

CONFIDENTIAL

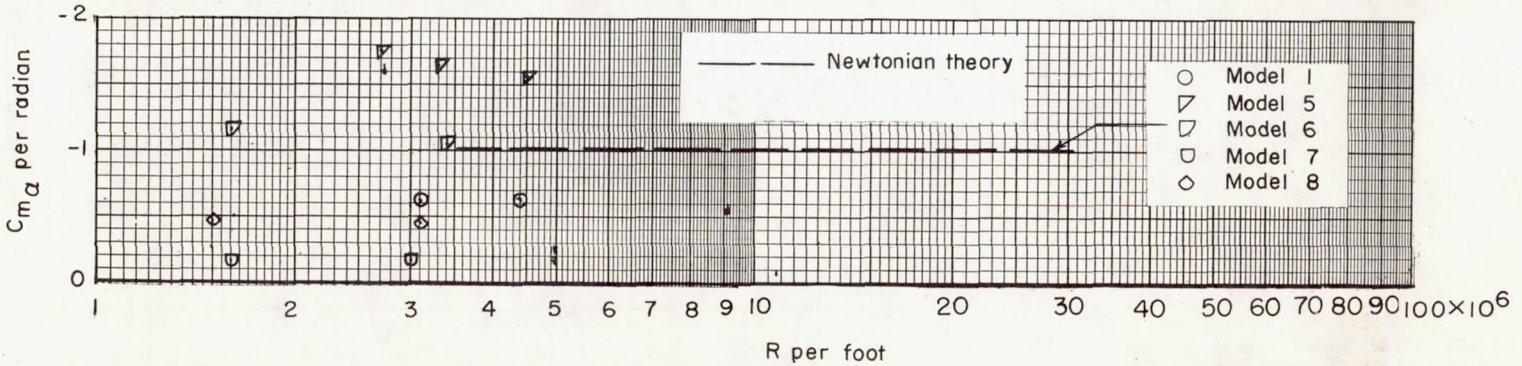


(b) M = 2.62.

Figure 6.- Continued.



(c) M = 4.06.



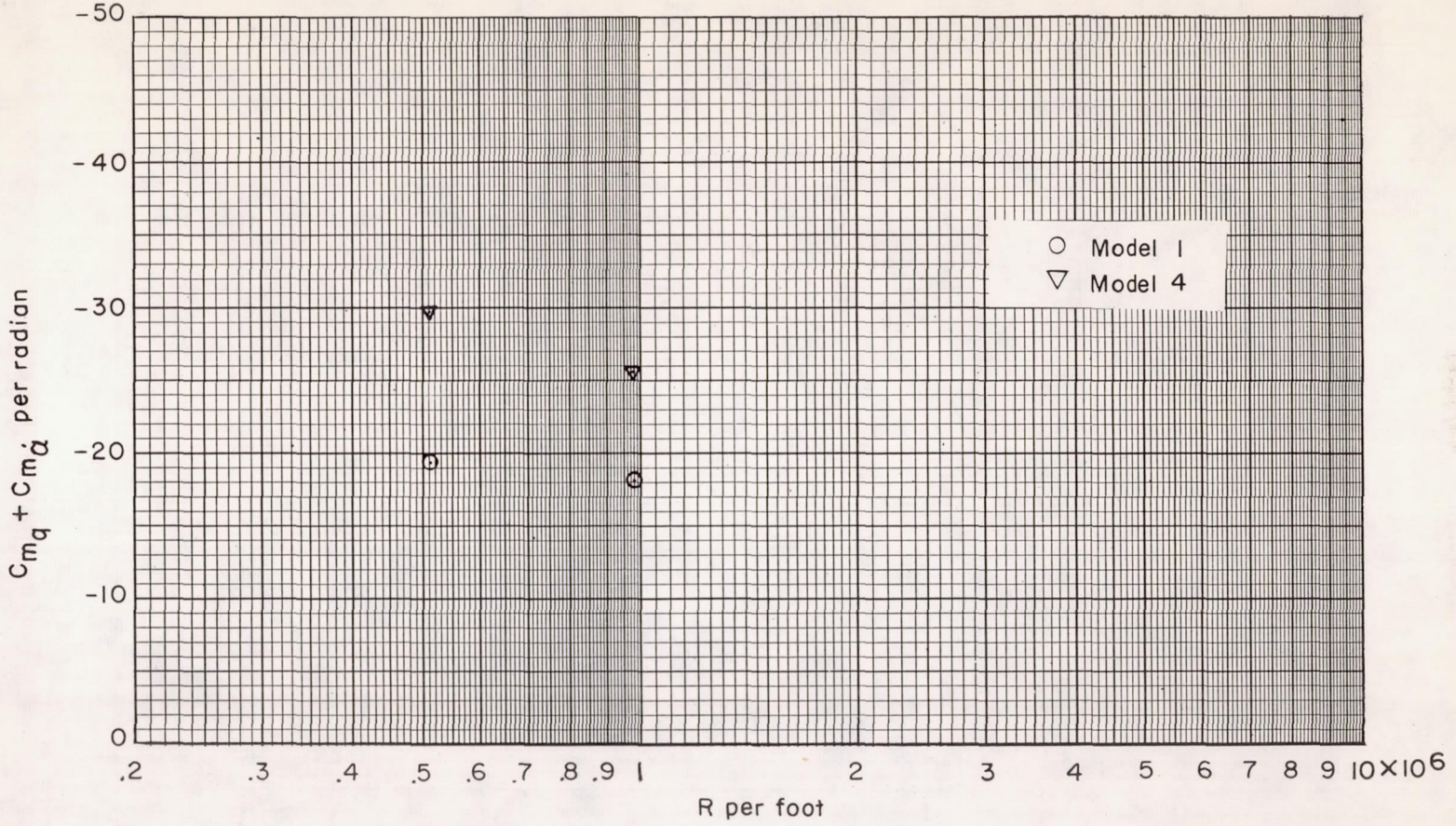
(d) M = 6.86.

Figure 6.- Concluded.

CONFIDENTIAL

CONFIDENTIAL

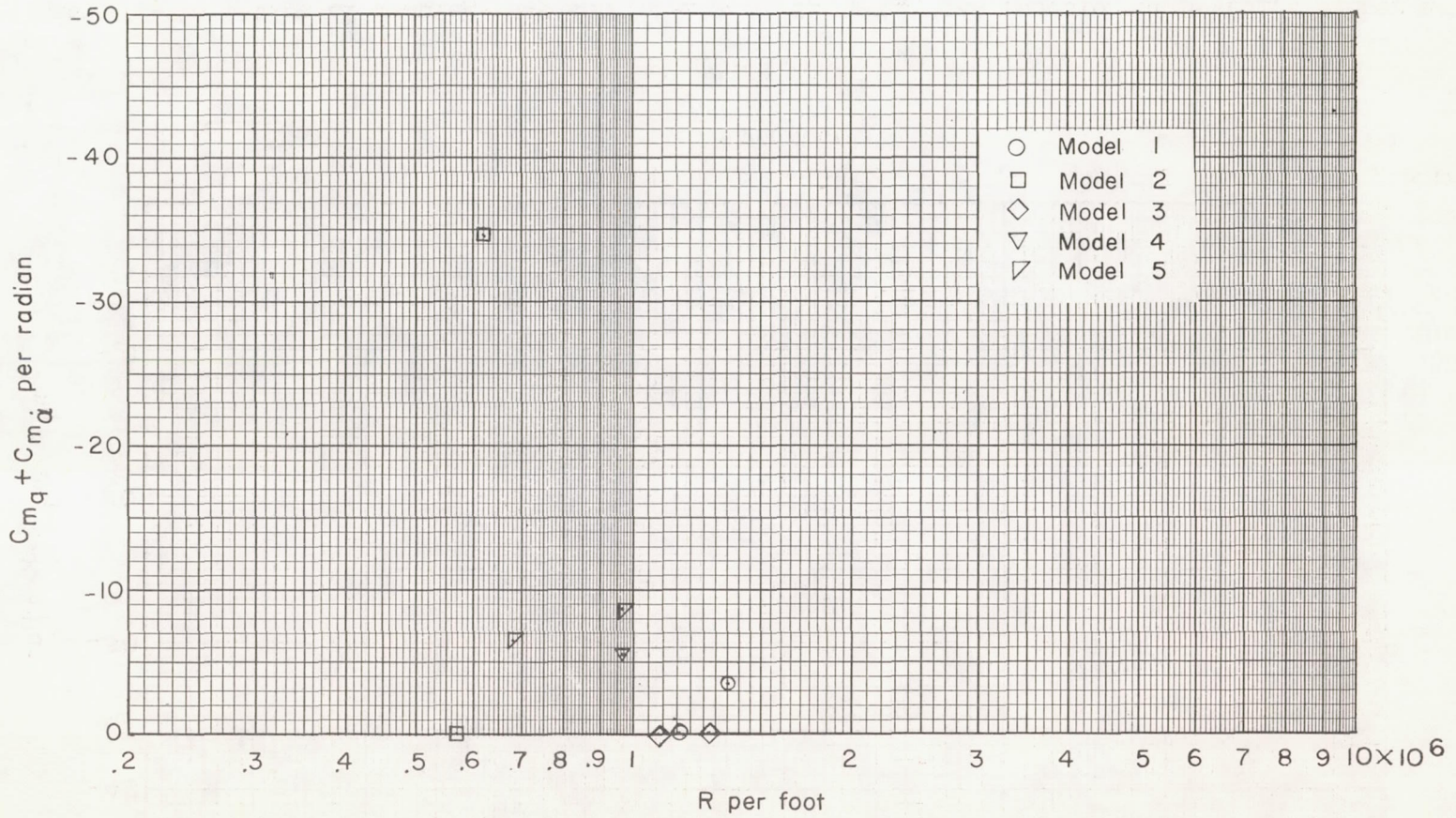
CONFIDENTIAL



(a) M = 1.62.

Figure 7.- Variation of damping-in-pitch parameter $C_{m_q} + C_{m_{\dot{\alpha}}}$ as function of Reynolds number at M = 1.62, 2.62, 4.06, and 6.86. Reference is base area and diameter of model 1.

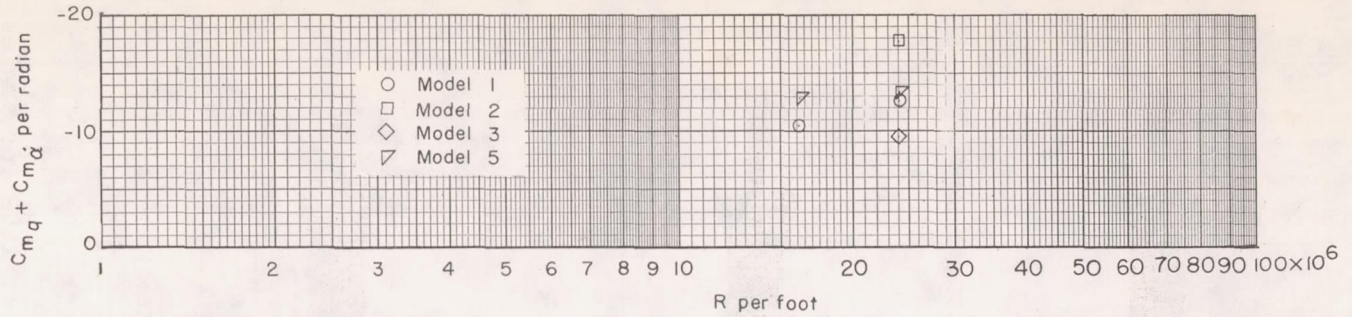
CONFIDENTIAL



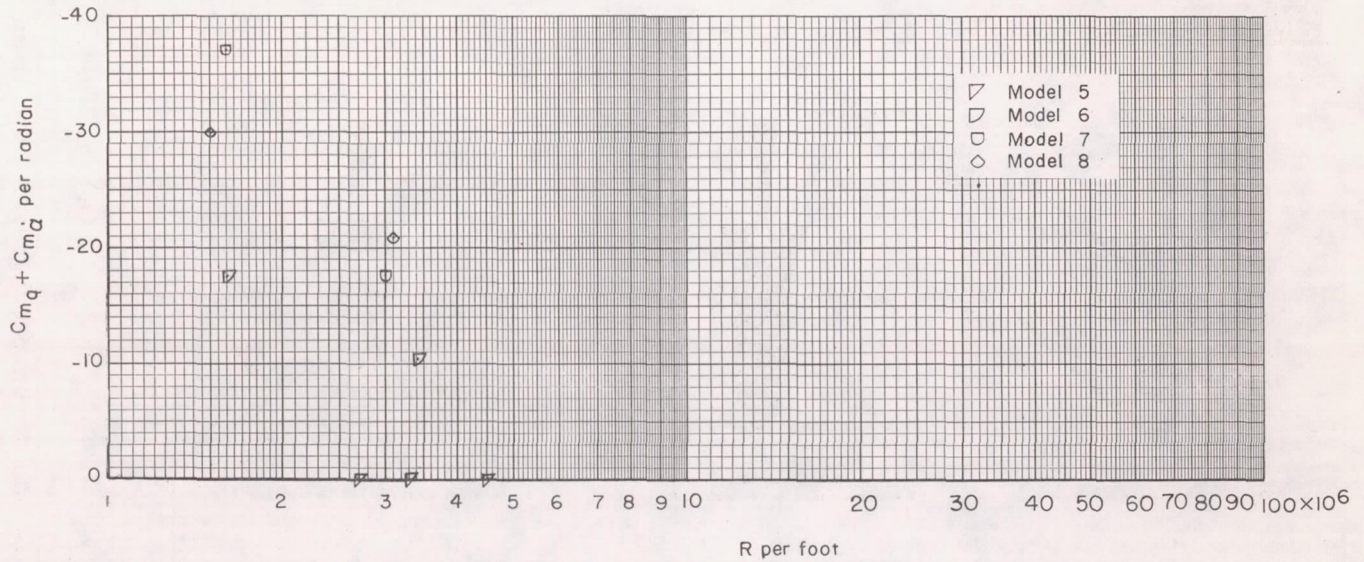
(b) M = 2.62.

Figure 7.- Continued.

CONFIDENTIAL

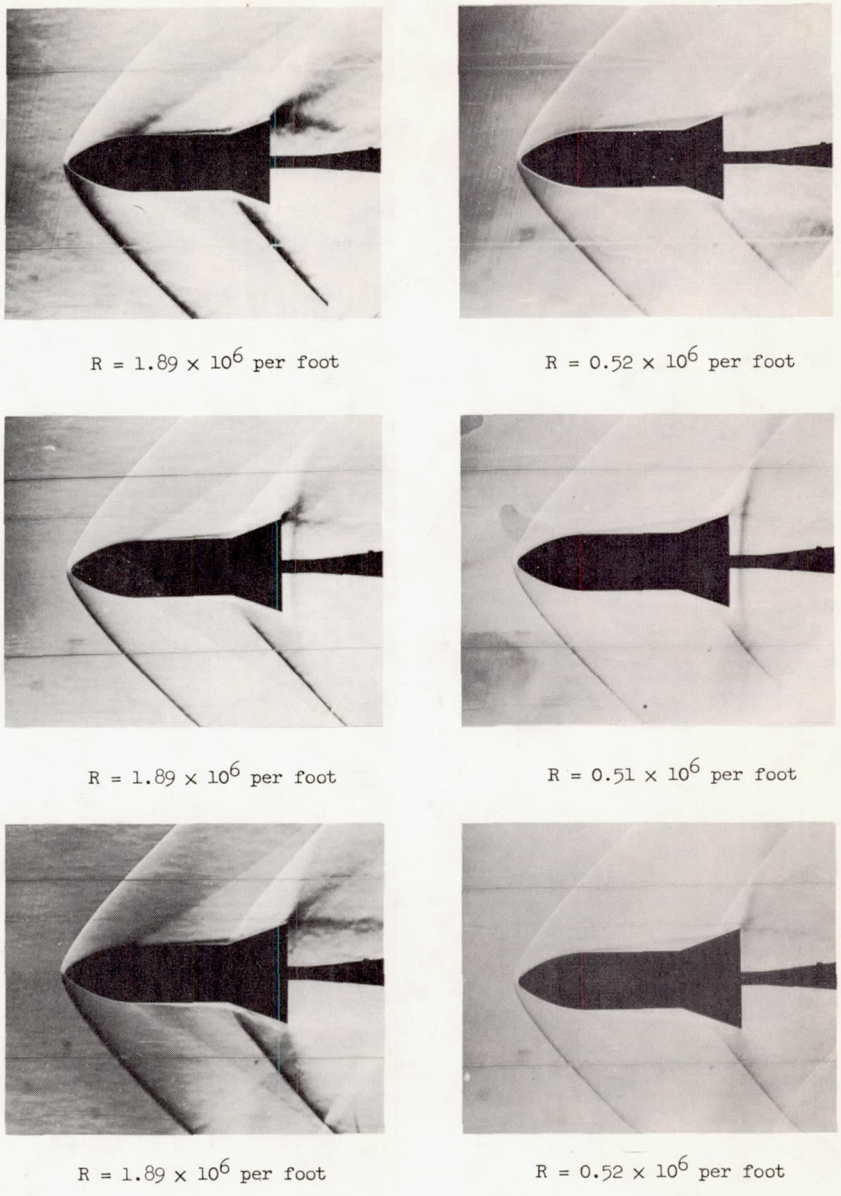


(c) M = 4.06.



(d) M = 6.86.

Figure 7.- Concluded.

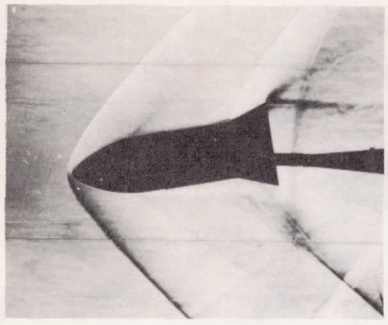


(a) $\alpha = 0^\circ$. L-57-2779

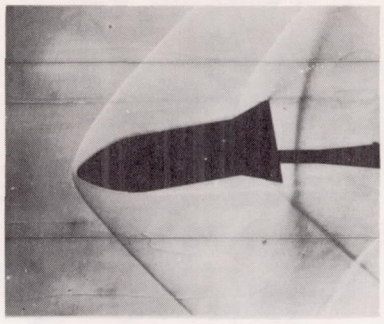
Figure 8.- Schlieren photographs at a Mach number of 1.62 for angles of attack of 0° and -10°.

DECLASSIFIED

Model 1

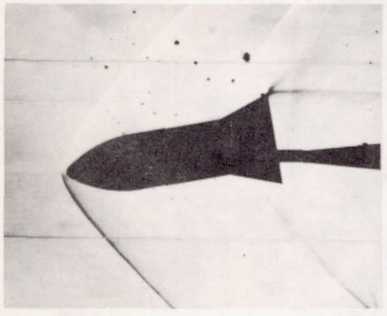


R = 1.89 × 10^6 per foot

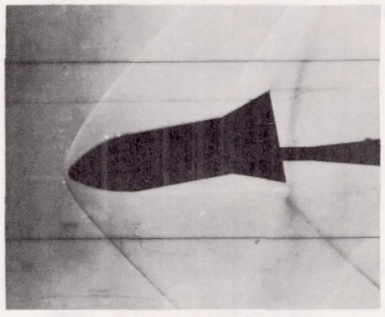


R = 0.52 × 10^6 per foot

Model 4

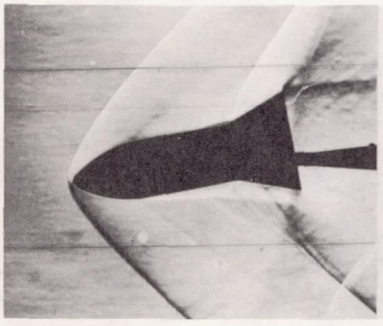


R = 1.89 × 10^6 per foot

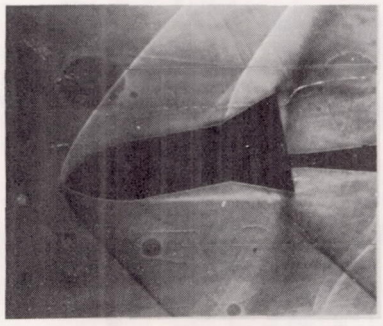


R = 0.53 × 10^6 per foot

Model 5



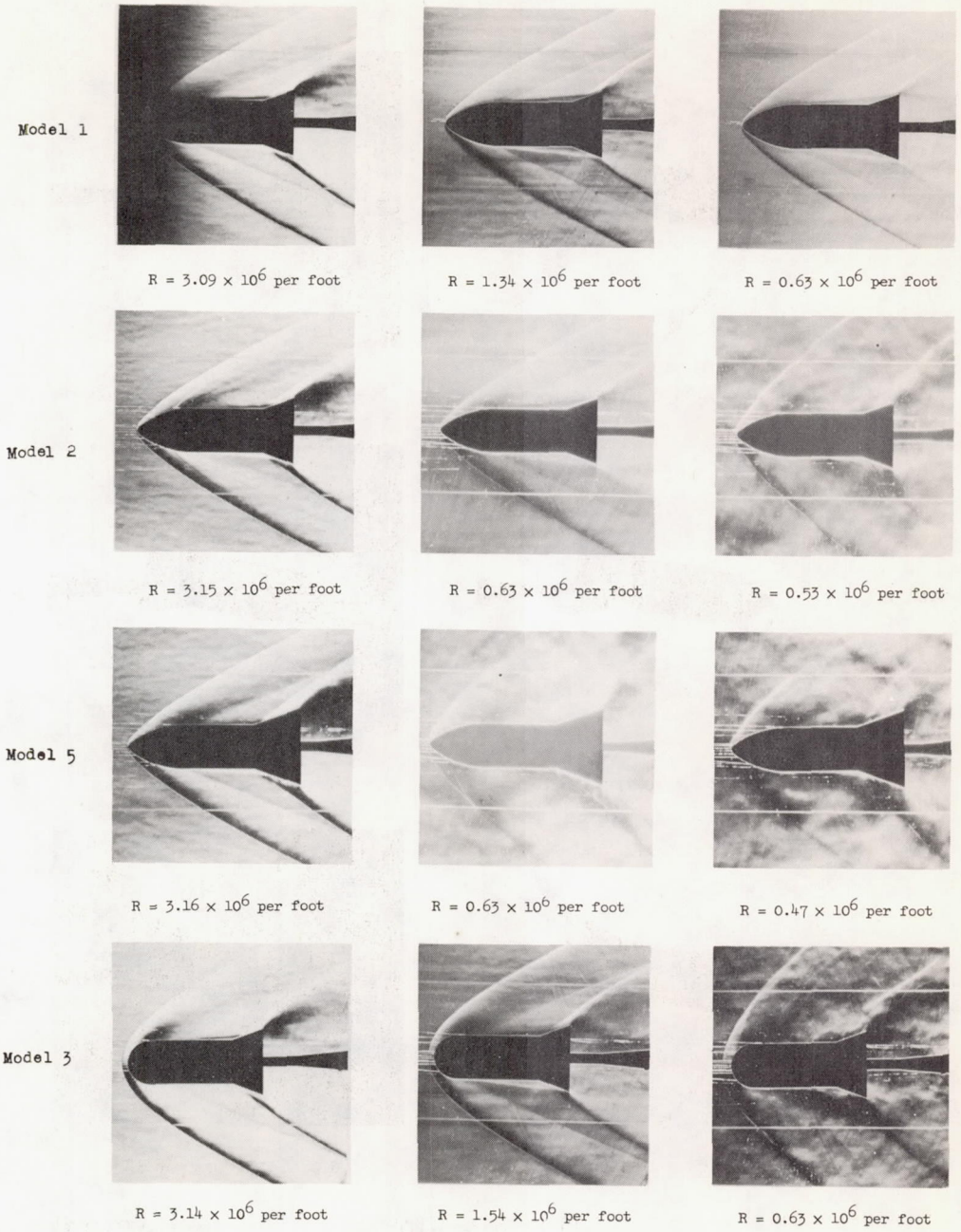
R = 1.89 × 10^6 per foot



R = 0.53 × 10^6 per foot

(b) $\alpha = -10^\circ$. L-57-2780

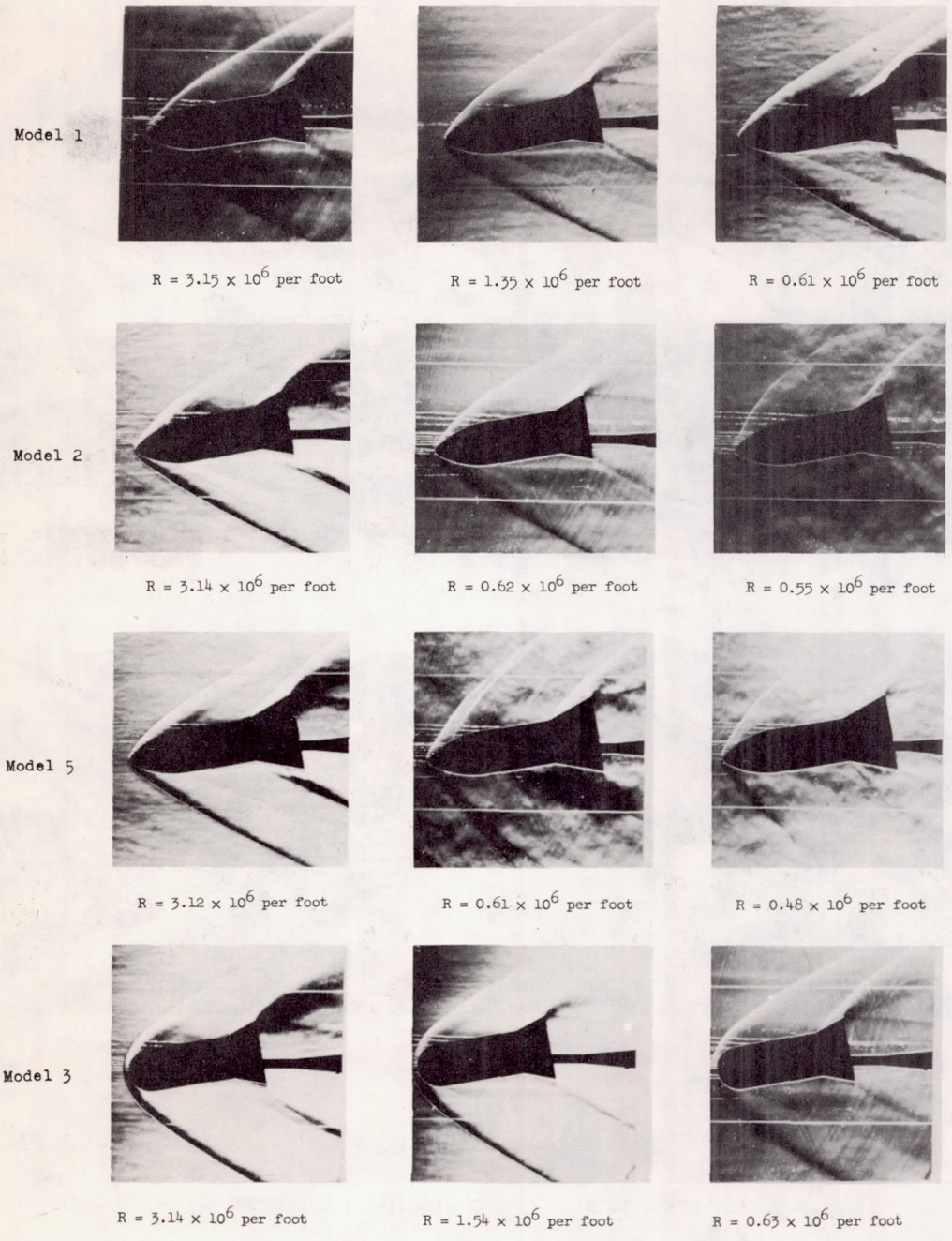
Figure 8.- Concluded.



(a) $\alpha = 0^\circ$. L-57-2781

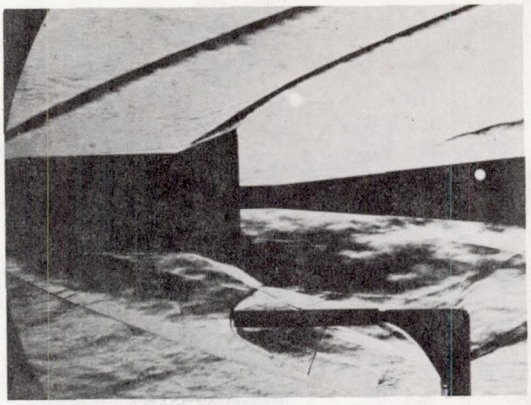
Figure 9.- Schlieren photographs at a Mach number of 2.62 for angles of attack of 0° and -10°.

DECLASSIFIED

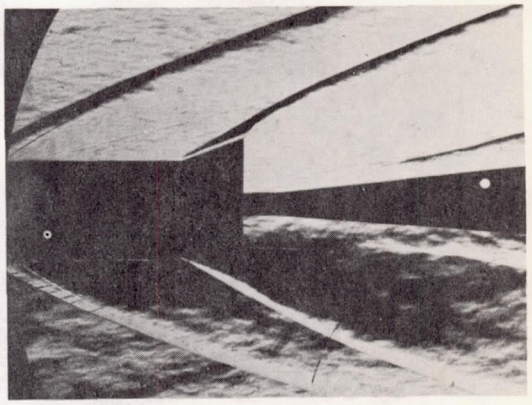


(b) $\alpha = -10^{\circ}$. L-57-2782

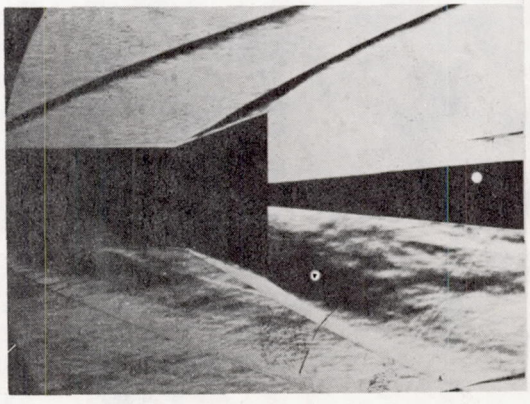
Figure 9.- Concluded.



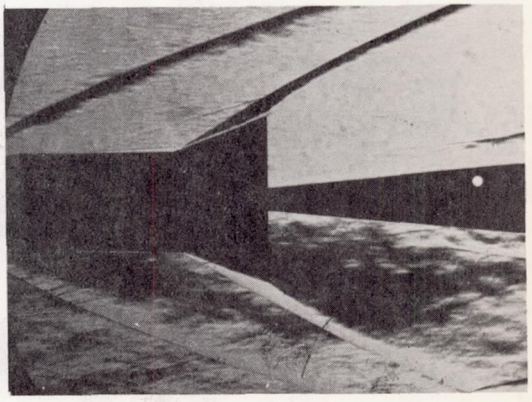
Model 1
$R = 17.2 \times 10^6$ per foot



Model 2
$R = 24.0 \times 10^6$ per foot



Model 5
$R = 17.2 \times 10^6$ per foot

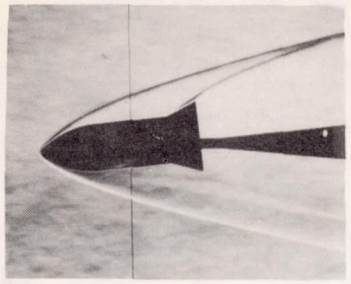


Model 5
$R = 24.0 \times 10^6$ per foot

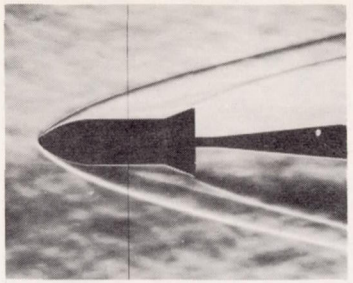
(a) M = 4.06. L-57-2783

Figure 10.- Schlieren photographs at Mach numbers of 4.06 and 6.86.

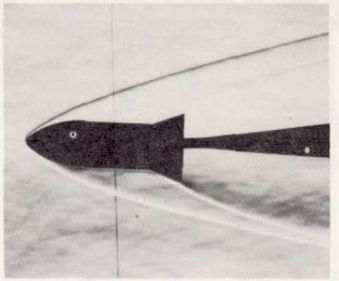
CONFIDENTIAL



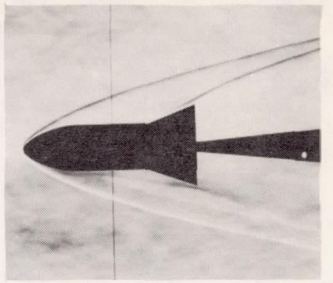
Model 1
$R = 3.1 \times 10^6$ per foot
$\alpha \approx -6^\circ$



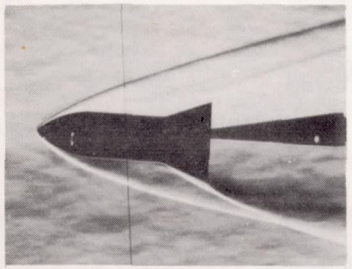
Model 1
$R = 3.1 \times 10^6$ per foot
$\alpha \approx 0^\circ$



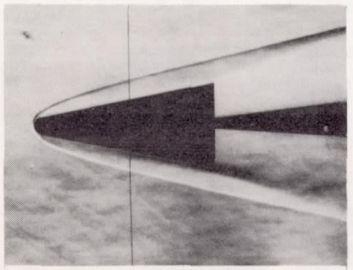
Model 1
$R = 4.4 \times 10^6$ per foot
$\alpha \approx 3^\circ$



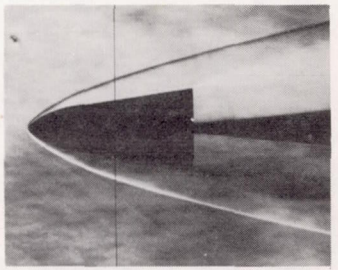
Model 5
$R = 2.7 \times 10^6$ per foot
$\alpha \approx -1^\circ$



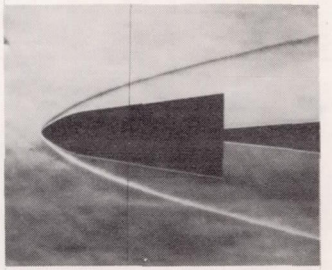
Model 5
$R = 4.5 \times 10^6$ per foot
$\alpha \approx 5^\circ$



Model 6
$R = 3.4 \times 10^6$ per foot
$\alpha \approx 0^\circ$



Model 7
$R = 3.0 \times 10^6$ per foot
$\alpha \approx 0^\circ$



Model 8
$R = 1.5 \times 10^6$ per foot
$\alpha \approx 0^\circ$

(b) M = 6.86.

L-57-2784

Figure 10.- Concluded.

CONFIDENTIAL

CONFIDENTIAL

CONFIDENTIAL

CONFIDENTIAL